THE JOURNAL OF BIOLOGICAL CHEMISTRY VOL. 287, NO. 28, pp. 23615–23625, July 6, 2012

Central Role of Mitofusin 2 in Autophagosome-Lysosome Fusion in Cardiomyocytes*[S]

Received for publication, May 7, 2012, and in revised form, May 22, 2012 Published, JBC Papers in Press, May 22, 2012, DOI 10.1074/jbc.M112.379164

Ting Zhao[‡], Xiaohu Huang[‡], Liang Han[‡], Xianhua Wang[‡], Hongqiang Cheng[§], Yungang Zhao[‡], Quan Chen[¶], Ju Chen[§], Heping Cheng[‡], Ruiping Xiao[‡], and Ming Zheng[‡1]

From the [‡]Institute of Molecular Medicine, State Key Laboratory of Biomembrane and Membrane Biotechnology, Peking-Tsinghua Center for Life Sciences, Peking University, Beijing 100871, China, the [§]Department of Medicine, University of California, San Diego, La Jolla, California 92093, and the [¶]Institute of Zoology, Chinese Academy of Sciences, Beijing 100101, China

Background: Mitofusin 2 is a mitochondrial outer membrane protein with multiple functions.
Results: Mitofusin 2 deficiency in the heart causes autophagosomes to accumulate and leads to cardiac dysfunction.
Conclusion: Mitofusin 2 serves as an adaptor protein to mediate the fusion of autophagosomes with lysosomes in the heart.
Significance: Mitofusin 2 has a novel and essential role in cardiac autophagic regulation.

In the heart, autophagy has been implicated in cardioprotection and ischemia-reperfusion tolerance, and the dysregulation of autophagy is associated with the development of heart failure. Mitochondrial dynamic proteins are profoundly involved in autophagic processes, especially the initiation and formation of autophagosomes, but it is not clear whether they play any role in cardiac autophagy. We previously reported that mitofusin 2 (MFN2), a mitochondrial outer membrane protein, serves as a major determinant of cardiomyocyte apoptosis mediated by oxidative stress. Here, we reveal a novel and essential role of MFN2 in mediating cardiac autophagy. We found that specific deletion of MFN2 in cardiomyocytes caused extensive accumulation of autophagosomes. In particular, the fusion of autophagosomes with lysosomes, a critical step in autophagic degradation, was markedly retarded without altering the formation of autophagosomes and lysosomes in response to ischemia-reperfusion stress. Importantly, MFN2 co-immunoprecipitated with RAB7 in the heart, and starvation further increased it. Knockdown of MFN2 by shRNA prevented, whereas re-expression of MFN2 restored, the autophagosome-lysosome fusion in neonatal cardiomyocytes. Hearts from cardiac-specific MFN2 knockout mice had abnormal mitochondrial and cellular metabolism and were vulnerable to ischemia-reperfusion challenge. Our study defined a novel and essential role of MFN2 in the cardiac autophagic process by mediating the maturation of autophagy at the phase of autophagosome-lysosome fusion; deficiency of MFN2 caused multiple molecular and functional defects that undermined cardiac reserve and gradually led to cardiac vulnerability and dysfunction.

Mitochondria are highly dynamic organelles, constantly undergoing shape changes controlled by fusion and fission. Mitochondrial fusion/fission-related proteins mainly consist of the fusion proteins mitofusin 1 and 2 (MFN1 and -2) and optic atrophy 1 (OPA1), and the fission proteins dynamin-related protein (DRP1) and FIS1 (1–5). Recent studies demonstrated that mitochondrial dynamic proteins are also associated with autophagy, a conserved process in all eukaryotes for self-degrading intracellular components and damaged organelles, to maintain normal organelle function and nutrient restoration (6–8). In addition, Parkin, an important player in Parkinson disease and a ubiquitin ligase related to mitochondrial fission by down-regulation of mitofusins, promotes autophagy to eliminate impaired mitochondria, thus providing a link between the clearance of dysfunctional mitochondria and the pathogenesis of neurodegenerative diseases (9). During starvation-induced autophagy, the mitochondrial outer membrane contributes to the formation of autophagosomes in a manner dependent on endoplasmic reticulum (ER)[2]/mitochondrial connections regulated by MFN2 (10). These studies indicate that mitochondrial dynamic proteins are profoundly involved in both the initiation of mitochondrial autophagy and the formation of autophagosomes. Nevertheless, little is known about the roles of mitochondrial dynamic proteins in the maturation of autophagosomes.

In a tissue with a high rate of aerobic metabolism, heart cells contain prominent mitochondrial networks, occupying up to 40% of the cell volume and generating ATP in response to energy needs through oxidative phosphorylation fueled by the catabolism of lipids and carbohydrates (11). Dysregulation of autophagy in response to Atg1 depletion is associated with the accumulation of deleterious mitochondria (12). However, whether mitochondria regulate autophagy in the heart has not yet been well defined. Unlike many other cell types, where mitochondria of irregular shape are highly mobile and prone to fusion-fission as pairs of mitochondria meet (13–15), the mitochondria in cardiomyocytes are restricted and immobilized in clusters between myofilaments (16). Nevertheless, mitochondrial fusion/fission proteins, especially MFN2, are expressed

* This work was supported by National Science Foundation of China Grants 30770870 and 30971062 and National Key Basic Research Program of China Grant 2007CB512100.
[S] This article contains supplemental Experimental Procedures, Figs. S1–S4, and additional references.
[1] To whom correspondence should be addressed. Tel.: 86-10-62757095; E-mail: zhengm@pku.edu.cn.

[2] The abbreviations used are: ER, endoplasmic reticulum; TEM, transmission electron microscopy; CKO, cardiac-specific knock-out.

abundantly in the heart (1). This raises the question of whether, in addition to regulating the mitochondrial fusion/fission process, these dynamically related proteins also play a role in mediating autophagic processes in the heart.

MFN2 was originally identified as a mitochondrial protein mediating fusion of the mitochondrial outer membrane, and mutation of *MFN2* is causally associated with Charcot-Marie-Tooth type 2A, a neurodegenerative disease (17, 18). In addition to mediating mitochondrial fusion, MFN2 localizes on the ER membrane, serving as a bridge to tether the ER to mitochondria (19). Moreover, MFN2 plays multiple roles in the regulation of cell metabolism, mitochondrial DNA stability, cell proliferation, and cell survival and death (20–23). The importance of MFN2 is manifested by the embryonic lethality of the global MFN2 knock-out mouse (24). Recently, the cardiac role of MFN2 has been explored *in vivo* in cardiac-specific MFN2 and MFN1/MFN2 knock-out mouse models (25, 26). Interestingly, cardiomyocytes lacking MFN2 have enlarged mitochondria and are protected from cell death due to the regulation of mitochondrial permeability transition pore opening in response to cardiac stresses (26). Conditionally combined MFN1/MFN2 ablation in adult mouse heart, however, leads to mitochondrial fragmentation and rapid cardiac failure (25). These studies suggest that although MFN1/MFN2-mediated mitochondrial fusion plays a pivotal role in regulating cardiac function, MFN2 may control cardiac function alternatively by a means independent of mitochondrial fusion.

Our previous studies have shown that up-regulation of MFN2 in response to oxidative stress triggers the apoptotic death of vascular smooth muscle cells and cardiomyocytes, whereas down-regulation or dysregulation of MFN2 leads to vascular proliferative disorders (22, 23, 27, 28). Here, we found a novel function of MFN2 in the heart. Our data showed that, in the cardiac-specific MFN2 knock-out mouse heart, MFN2 deficiency impaired autophagosome-lysosome fusion, and the subsequent accumulation of autophagosomes in cardiomyocytes eventually led to cardiac dysfunction.

EXPERIMENTAL PROCEDURES

Animal Handling—All procedures of animal handling were approved by the Institutional Animal Care and Use Committee at Peking University and by AAALAC International. The *Mfn2* gene exon 4 floxed mice ($Mfn2^{f/f}$) were generated by standard techniques and were bred with *Mlc2v*-Cre mice to generate cardiac-specific MFN2 knock-out mice (MFN2 CKO), as described previously (29). Mice were anesthetized with 10% chloral hydrate, and the hearts were excised for transmission electron microscopy assay, RT-PCR, Western blot, histology, and immunofluorescence detection. In the starvation experiments, 4-month-old mice were deprived of food for 2 days but had free access to drinking water. Detailed procedures are in the supplemental material.

Transmission Electron Microscopy—After anesthesia, mice were fixed with 2% paraformaldehyde and 2.5% glutaraldehyde in 0.1 M PBS (pH 7.4), and the hearts were excised, post-fixed, dehydrated, and then embedded in epoxy resin. Ultra-thin sections (70–90 nm) were observed with a transmission electron microscope (JEM-1010, JEOL).

Isolation, Culture, and Adenovirus Transfection of Neonatal and Adult Cardiomyocytes—Neonatal and adult cardiomyocytes were enzymatically isolated and cultured as described previously (23, 30). Adenoviruses containing GFP-LC3, MFN2-GFP, MFN2 cDNA, and MFN2-shRNA were used to infect neonatal and adult cardiomyocytes. Cells were harvested to assess the efficiency of gene knockdown by Western blotting or prepared for functional studies. Mouse MFN2 cDNA was from Invitrogen. Adenoviruses expressing GFP-LC3 and MFN2 were packaged using the Stratagene Adeasy system following the procedures provided. Two sets of MFN2-shRNA were designed to specifically target rat MFN2, with the sequences 5′-GGACCCAGTTACTACAGAAGA-3′ and 5′-GCTCCTGGCTCAAGACTATAA-3′. The MFN2-shRNA was packaged into adenovirus using the BLOCK-iT™ adenoviral RNAi expression system (Invitrogen).

Western Blot and Co-immunoprecipitation— Protein was extracted from mouse hearts and separated by SDS-PAGE. The transferred PVDF membranes were probed with the primary antibodies (anti-LC3B, anti-RAB7, and anti-tubulin from Sigma; anti-FYCO1 from Novus; anti-p62 from MBL; and anti-phospho-eIF2α and anti-eIF2α from Cell Signaling) and then incubated with the secondary antibodies (IRDye-conjugated anti-mouse and anti-rabbit IgG from LI-COR). Immunoblots were evaluated using the Odyssey imaging system.

For co-immunoprecipitation, the whole heart lysate was precleaned with protein A/G (Santa Cruz Biotechnology) and incubated with anti-RAB7 (Sigma), anti-MFN2 (Abnova), or control IgG for 3 h; protein A/G was then added, and samples were shaken at 4 °C overnight. The precipitates were washed three times with PBS, and the proteins were denatured for Western blot.

Isolation of Cardiac Mitochondria and Functional Assay—Cardiac mitochondria were isolated as described previously (31), and mitochondrial respiratory function was evaluated by measuring oxygen consumption. Detailed procedures are in the supplemental material.

Ischemia Reperfusion Model—The heart was rapidly excised, and the aorta was cannulated and perfused with Tyrode solution containing 2 mM $CaCl_2$ at a constant pressure of 80 mm Hg, equilibrated with 95% O_2 and 5% CO_2, and maintained at 37 °C. After stabilization for 20 min, the heart was subjected to 30 min of ischemia followed by 30 min of reperfusion. For autophagic flux assay, hearts were perfused with Tyrode solution containing either a combination of 5 μg/ml pepstatin A (Sigma) and 30 mM NH_4Cl (Sigma) or DMSO as solvent control. Ventricular myocardium was harvested, and total protein was extracted for Western blot.

For measurement of $\Delta\Psi_m$, the heart was perfused with Tyrode solution containing 100 nM tetramethylrhodamine methyl ester (Invitrogen) and 10 nM blebbistatin (Sigma). Confocal images were taken from multiple randomly selected regions before and after I/R. Each image was taken ~30 μm deep into the epimyocardium of the left ventricle. The same procedure was performed for detection of functional lysosomes by perfusing with Tyrode solution containing 50 nM LysoTracker™ red (Invitrogen). To quantify the lysosome produc-

tion, the percentage surface area covered by LysoTracker™ red was measured using ImageJ software.

Statistical Analysis—Data are reported as mean ± S.E. The unpaired *t* test with repeated measures was applied, when appropriate, to determine the statistical significance of differences. $p < 0.05$ was considered statistically significant.

RESULTS

Cardiac Deficiency of MFN2 Leads to Accumulation of Autophagosomes in Cardiomyocytes—The cardiac MFN2 knock-out mouse model (CKO) was generated to specifically study the cardiac function of MFN2 (supplemental Fig. S1). Interestingly, although MFN2 depletion in mouse embryonic fibroblasts by adenovirus-mediated Cre transfection (supplemental Fig. S2*A*) led to mitochondrial fragmentation as expected (supplemental Fig. S2*B*), knock-out of MFN2 in cardiomyocytes resulted in increased numbers of large mitochondria (supplemental Fig. S3*A*) and an average 61.5% increase in individual mitochondrial area, from 0.65 μm^2 in control heart to 1.05 μm^2 in MFN2 CKO heart from micrographs of transmission electron microscopy (TEM) sections (supplemental Fig. S3*B*). However, no significant change of total mitochondrial mass was found in the MFN2 CKO mouse heart, as indicated by unaltered mitochondrial volume density and mtDNA copy number (supplemental Fig. S3, *C* and *D*). Moreover, the CKO heart showed no difference in the deletion containing NADH dehydrogenase subunit 4 (ND4), a common feature of diseased and aging hearts (32, 33), compared with control heart (supplemental Fig. S3*D*). Indeed, the relative frequency of mitochondrial area distribution shifted to the right, showing an increased proportion of large mitochondria in the population (supplemental Fig. S3*E*). These results are thus in general agreement with a recently published study in which enlarged mitochondria were described in the heart of a different MFN2 cardiac knock-out mouse model (26). These data from MFN2 knock-out hearts indicate that MFN2 plays roles other than mediating mitochondrial fusion in the heart.

Surprisingly, the TEM data revealed a large number of double and multimembrane autophagosome-like vacuolar structures in the MFN2 CKO heart (Fig. 1*A*). To confirm that MFN2 depletion is associated with abnormal autophagic activity, the conversion of the soluble form of LC3 (LC3-I) to the lipidated and autophagosome-associated form (LC3-II), the hallmark of autophagic processing at the molecular level, was measured (34). A 1.97-fold increase of LC3-II protein level was found in the MFN2 CKO heart over that from wild-type littermate heart (Fig. 1*B*). Furthermore, immunohistochemical staining of MFN2 CKO heart sections with LC3 antibody showed accumulated LC3-positive staining (Fig. 1*C*), and immunofluorescent staining of single cardiomyocytes isolated from the CKO heart also showed elevated LC3-positive puncta (Fig. 1*D*), consistent with the notion that LC3-II protein accumulates in autophagosomal membranes, whereas LC3-I is localized in the cytosol in a soluble form (34, 35). These data suggest that the depletion of MFN2 in heart leads to the increased accumulation of autophagosomes.

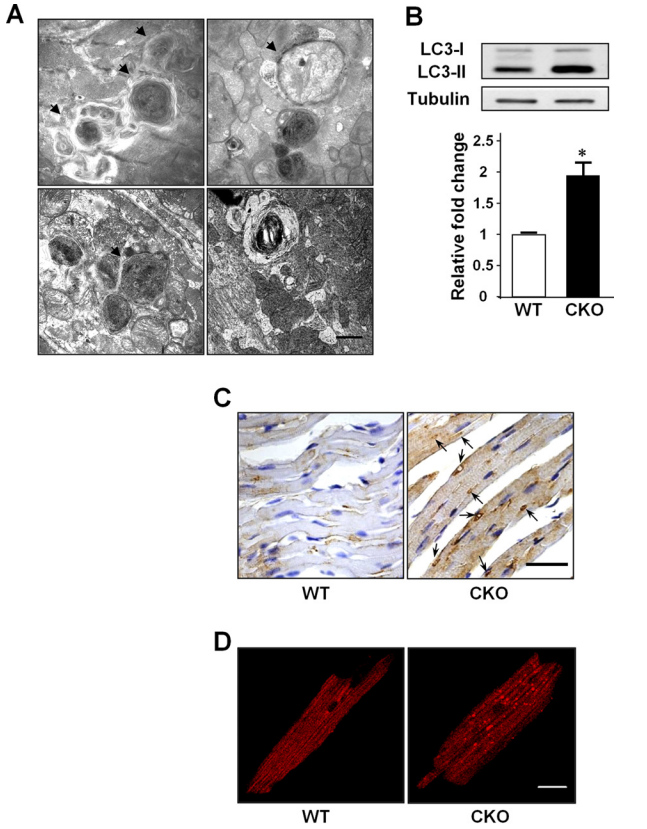

FIGURE 1. **MFN2 depletion causes autophagosome accumulation.** *A,* representative multimembrane structures (*arrows*) and autophagic vacuoles (*arrowheads*) in CKO mouse heart at 4 months of age by TEM. *Scale bar,* 1 μm. *B,* increased LC3-II level. $n = 3$ pairs. *C,* immunohistochemical staining of endogenous LC3 in wild-type and CKO heart. *Scale bar,* 50 μm. *D,* immunofluorescence staining of endogenous LC3 in isolated wild-type and CKO cardiomyocytes. *Scale bar,* 20 μm. *, significant difference between wild-type and MFN2 CKO hearts.

Depletion of MFN2 Impairs Autophagosome-Lysosome Fusion in the Heart—Autophagy is a highly regulated process, which includes the formation of autophagosomes with sequestration of cytosolic proteins or organelles, the fusion of autophagosomes with lysosomes to generate autophagolysosomes, and the degradation of the cargo in autophagolysosomes by lysosomal proteases (36). The question raised here is whether the accumulation of autophagosomes in response to MFN2 depletion is mainly due to the increased formation of autophagosomes or a consequence of an impaired autophagic degradation process. To address this question, we first assessed the expression levels of p62 protein, a specific autophagic substrate protein representing autophagic flux (37). Compared with wild-type littermates, hearts from MFN2 CKO mice showed a 2.09-fold increase in p62 level (Fig. 2*A*), indicating impaired autophagic degradation due to defects of autophagosome turnover. To further evaluate the dynamic autophagic process in the MFN2 CKO mouse heart, the combination of two lysosomal inhibitors, NH_4Cl and pepstatin A, was introduced into Langendorff-perfused hearts to interrupt the degradation of autophagosomes. Inhibition of lysosomes by these compounds led to the accumulation of autophagosomes in wild-type mouse heart, as indicated by increased levels of LC3-II (Fig. 2*B*). In sharp contrast, LC3-II protein in MFN2

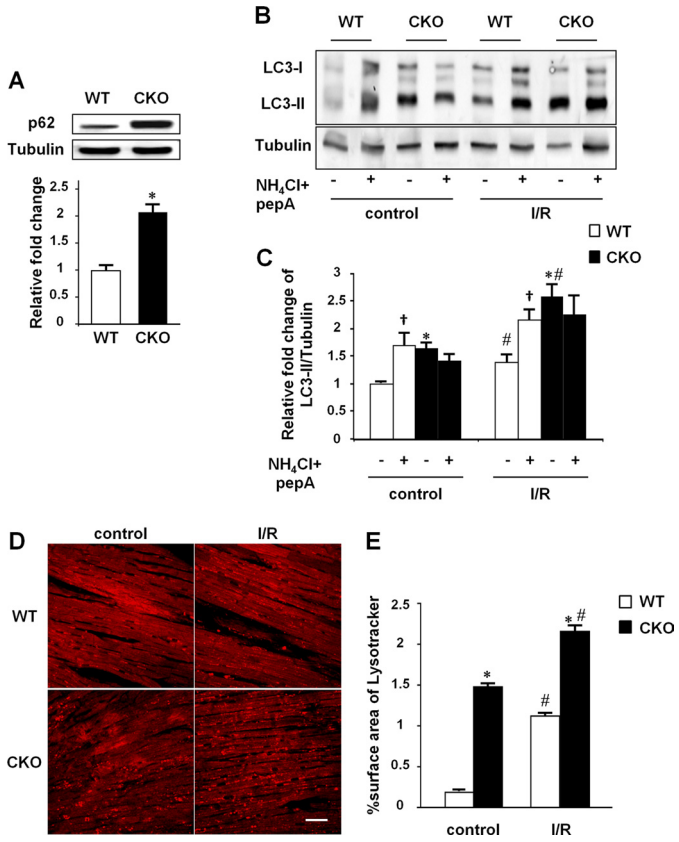

FIGURE 2. **Defective autophagic degradation in MFN2 CKO heart.** *A,* increased p62 level by Western blot and statistics of the p62/tubulin ratio. $n = 3$ pairs of wild-type control and MFN2 CKO mice at 4 months old. *B,* LC3-II protein levels showing the autophagic flux determined by Western blot in Langendorff-perfused hearts under ischemia-reperfusion stress (IR) with or without the lysosomal inhibitors NH_4Cl and pepstatin A. *C,* LC3-II/tubulin ratios from *B*. $n = 3$ for each group. *D,* confocal images of Langendorff-perfused hearts stained by LysoTracker™ red before and after ischemia-reperfusion stress. *E,* surface area of LysoTracker™ red staining counted from *D*. *, significant difference between wild-type and MFN2 CKO hearts; †, significant difference between inhibitor-treated and untreated groups; #, significant difference between ischemia-reperfusion (I/R)-treated and untreated groups.

CKO mouse heart, already at higher levels than control littermates in the basal condition, failed to respond to NH_4Cl and pepstatin A (Fig. 2, *B* and *C*). Similar results were also obtained in hearts treated with the autophagosome-lysosome fusion inhibitor bafilomycin A (data not shown), strongly suggesting an impairment of autophagosome-lysosome fusion in the MFN2-deficient heart. Next, we investigated the capacity for autophagosome formation in MFN2 knock-out hearts by performing ischemia-reperfusion, a well known autophagy-inducing stress (38). Hearts from both wild-type control and MFN2 CKO mice displayed elevated autophagosome activity in response to ischemia-reperfusion stress, as indicated by LC3-II protein levels, to a 1.38-fold increase in wild-type and a 1.56-fold increase in MFN2 CKO, compared with untreated hearts (Fig. 2, *B* and *C*). In the presence of ischemia-reperfusion stress, NH_4Cl and pepstatin A further increased the accumulation of autophagosomes in hearts from wild-type littermates but had no further effect on MFN2 CKO hearts (Fig. 2, *B* and *C*), supporting our hypothesis that MFN2 depletion in the heart impairs autophagosome degradation without affecting their formation.

In addition to the formation of autophagosomes, the capacity for lysosome formation, another factor that affects the degradation process of autophagy, was measured in Langendorff-perfused intact hearts. The heart was loaded with 50 nM LysoTracker™, an indicator of lysosomes, for 10 min. Confocal imaging revealed increased lysosome fluorescence, as indicated at 543 nm excitation, to a density of 1.48% surface area in MFN2 CKO mouse hearts, compared with the 0.18% surface area in wild-type control hearts (Fig. 2, *D* and *E*), indicating an increased propensity of MFN2-null cardiomyocytes to degrade the accumulated autophagosomes. Ischemia-reperfusion stress further increased lysosome density to 2.15 and 1.12%, in MFN2 CKO and wild-type hearts, respectively (Fig. 2, *D* and *E*), suggestive of an unimpaired capacity for lysosome formation in MFN2-deficient hearts in response to stress. Taken together, these *ex vivo* results indicate that MFN2 depletion impairs the degradation of autophagosomes without affecting the formation of either autophagosomes or lysosomes.

MFN2 Depletion Triggers ER Stress in Cardiomyocytes—MFN2 was recently reported to reside not only on the mitochondrial outer membrane but also on the ER membrane, facilitating the fine regulation of calcium homeostasis between the ER and mitochondria (19). So, we then examined the localization of MFN2 in adult cardiomyocytes by expressing MFN2-GFP fusion protein and loading the cells with the mitochondrial indicator MitoTracker™ red. Although confocal imaging showed the mitochondrial localization of MFN2 as indicated by the co-localization of green fluorescence from MFN2-GFP with the red fluorescence of MitoTracker™ red, MFN2 was mainly distributed at the ends of mitochondria where the ER and mitochondria contact (Fig. 3*A*). TEM analysis of adult cardiomyocytes confirmed the structural basis of the close contact between ER and mitochondria (data not shown). Next, we simultaneously loaded isolated adult cardiomyocytes from either control or MFN2 CKO mouse heart with ER-Tracker™ and MitoTracker™ to visualize the ER and mitochondria, respectively. Compared with the uniform pattern of ER-Tracker™ in control cardiomyocytes, increased fluorescence of ER-Tracker™ was detected in MFN2-deficient cells surrounding cavities lacking MitoTracker™ staining (Fig. 3*B*), pointing to the possibility that MFN2 depletion causes stressed ER and dysfunctional mitochondria. To test this, we analyzed the mRNA levels in control and MFN2 CKO hearts by RT-PCR and found an overall increase in the ER stress-related genes *Asns, Atf4, Trib3, Chop, Atf6*, and *Gsta1*, in the CKO hearts (Fig. 3*C*). In addition, phosphorylation of eukaryotic initiation factor 2α (eIF2α), a substrate of activated PRK-like ER kinase in response to increased ER stress, was also elevated in the CKO hearts (Fig. 3*D*), supporting the idea of increased ER stress signals consequential to MFN2 depletion in the heart.

Next, to clarify whether the accumulation of autophagosomes was merely a consequence of increased ER stress, a potent autophagy trigger, in response to MFN2 depletion, we measured the merging of autophagosomes with lysosomes in neonatal cardiomyocytes. Cells were transfected with adeno-GFP-LC3 to show the autophagosome signal, stained with LysoTracker™ to show the lysosome signal, and then treated with the ER stress inducers, thapsigargin and tunicamycin.

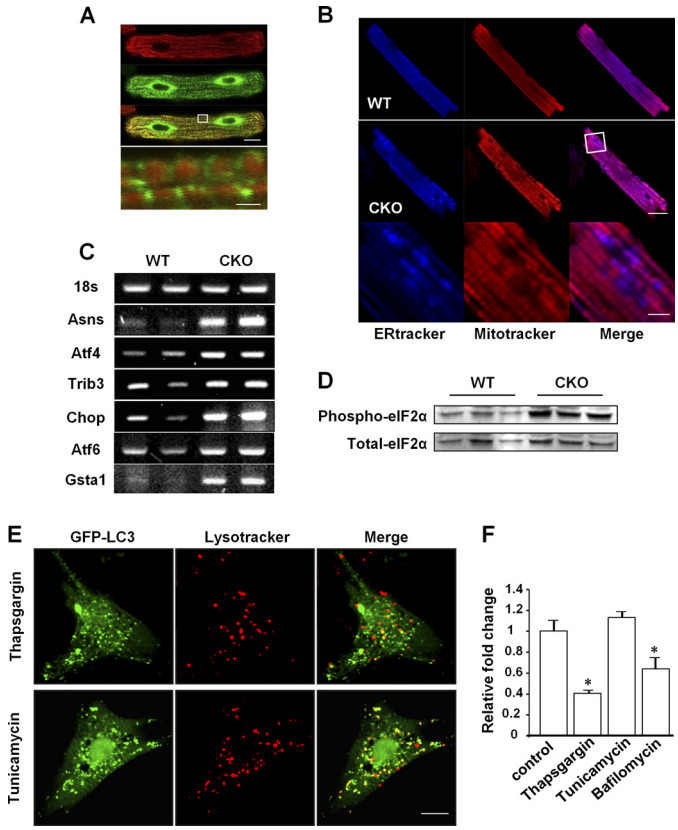

FIGURE 3. **MFN2 depletion increases ER stress signals.** *A,* confocal images of adult cardiomyocytes transfected with Ad-MFN2-GFP for 48 h and then loaded with MitoTracker. *Scale bars* are as follows: 10 μm for the whole cell and 1 μm for the high magnification view. *B,* cardiomyocytes from control (*upper*) and MFN2 CKO (*middle*) mouse heart stained with ER-Tracker™ and MitoTracker™. High magnification views (*bottom*) of ER-Tracker™ staining in MFN2 CKO cardiomyocytes. *Scale bars* are as follows: 20 μm for top and middle and 5 μm for bottom. *C,* mRNA levels of ER stress-related genes. *D,* expression of phospho-eIF2α and total-eIF2α in wild-type and CKO hearts. *E,* confocal images of neonatal cardiomyocytes transfected with Ad-GFP-LC3, treated with 1 μM thapsigargin or 5 μg/ml tunicamycin for 5 h, and loaded with LysoTracker™ for 10 min before imaging. *F,* relative fold change of merged LC3 dots and LysoTracker™ dots in cells treated with thapsigargin (1 μM), tunicamycin (5 μg/ml), or bafilomycin A1 (50 nM) compared with cells treated with DMSO. $n = 35$ cells for each group from three independent experiments. *, significant difference between control and treated cells.

Although both stress-inducers increased the numbers of autophagosomes in neonatal cardiomyocytes, as shown by increased numbers of GFP-LC3 puncta, the percentage of autophagosomes merged with lysosomes in total autophagosomes showed no difference in tunicamycin-treated cells (Fig. 3, *E* and *F*). In sharp contrast, thapsigargin and the autophagosome-lysosome fusion inhibitor bafilomycin A dramatically reduced the percentages of the autophagosomes merged with lysosomes by 59.5 and 35.8% compared with control cardiomyocytes (Fig. 3, *E* and *F*). In addition to a potent ER stressor, however, thapsigargin itself has been shown to directly impair autophagosome-lysosome fusion by blocking the recruitment of RAB7 to autophagosomes even in the ER stress-deficient mouse embryonic fibroblasts (39). Together, our data provide evidence that MFN2 depletion triggers ER stress in the heart, but the increased ER stress *per se* has no effect on the fusion of autophagosomes with lysosomes, thus further suggesting that the impairment of autophagosome-lysosome fusion in MFN2-deficient cardiomyocytes is due to MFN2 depletion but is not a consequence of ER stress.

MFN2 Is Required for Autophagosome-Lysosome Fusion and Interacts with RAB7—To demonstrate the causal role of MFN2 depletion in the impaired autophagosome-lysosome fusion, we transiently transfected cultured neonatal rat cardiomyocytes with adenovirus containing MFN2 shRNA to down-regulate, and MFN2 cDNA to restore, the MFN2 protein level. Two sets of shRNAs (MFN2-shRNA1 and MFN2-shRNA2) effectively down-regulated MFN2 protein by 62.4 and 74.6%, as compared with scrambled control, and co-transfection of MFN2 cDNA with MFN2 shRNA2 largely restored MFN2 protein to the control level (Fig. 4*A*). The merging of autophagosomes with lysosomes was then measured by transfecting the cells with adeno-GFP-LC3 and staining with LysoTracker™. Knockdown of MFN2 by shRNA2 significantly diminished the percentage of autophagosomes merged with lysosomes, from 25.5% in scrambled control to 5.9% in MFN2 knockdown cardiomyocytes (Fig. 4, *B* and *C*), whereas re-expression of MFN2 largely restored the level to 18.3% (Fig. 4, *B* and *C*). Similarly, rapamycin, a stimulator of autophagy, while increasing the numbers of autophagosomes and lysosomes, caused parallel changes to the merged autophagosomes-lysosomes in response to MFN2 knockdown or restoration (Fig. 4*D*). The ratio of autophagosomes merged with lysosomes by rapamycin was decreased to 12.0% in the presence of MFN2-shRNA2 and recovered to 26.0% with co-expression of MFN2 cDNA, compared with scrambled control at a ratio of 30.1% (Fig. 4*D*). Thus, our data indicate that MFN2 is necessary for the fusion of autophagosomes with lysosomes in cardiomyocytes.

Because MFN2 resides on the ER membrane, which is one of the major origins of autophagosome membrane, we hypothesized that MFN2 serves as an adaptor on ER-derived autophagosome membrane to mediate the fusion of autophagosomes with lysosomes. We then measured the protein levels of FYCO1 and RAB7, two mammalian autophagosome maturation-related proteins (40–42), but we found no difference between control and MFN2 CKO mouse hearts (Fig. 4*E*). However, immunoprecipitation experiments showed an interaction between MFN2 and RAB7, the small GTP-binding protein needed for the final maturation of late autophagic vacuoles (40, 41). Furthermore, control mice were subjected to starvation for 2 days to elevate cardiac autophagy. Interestingly, although both MFN2 and RAB7 protein levels were not changed in response to starvation, the interaction of MFN2 with RAB7 was significantly increased (Fig. 4*F*). These results suggest that MFN2 mediates the maturation of autophagy in the heart by serving as an adaptor protein recruiting RAB7 to the autophagosomal membrane.

MFN2 Knock-out Disturbs Cellular and Mitochondrial Metabolism and Causes Late Onset Cardiac Dysfunction and Increased Vulnerability to Ischemia Reperfusion Injury—Defective autophagy is known to impair the restoration of cellular nutrients and homeostasis, thus compromising cell function (43, 44), so we tested whether the autophagic impairment induced by MFN2 deletion causes metabolic dysfunction in cardiomyocytes. Because the heart is a lipid-consuming tissue, we first investigated the impact of MFN2-mediated autophagic

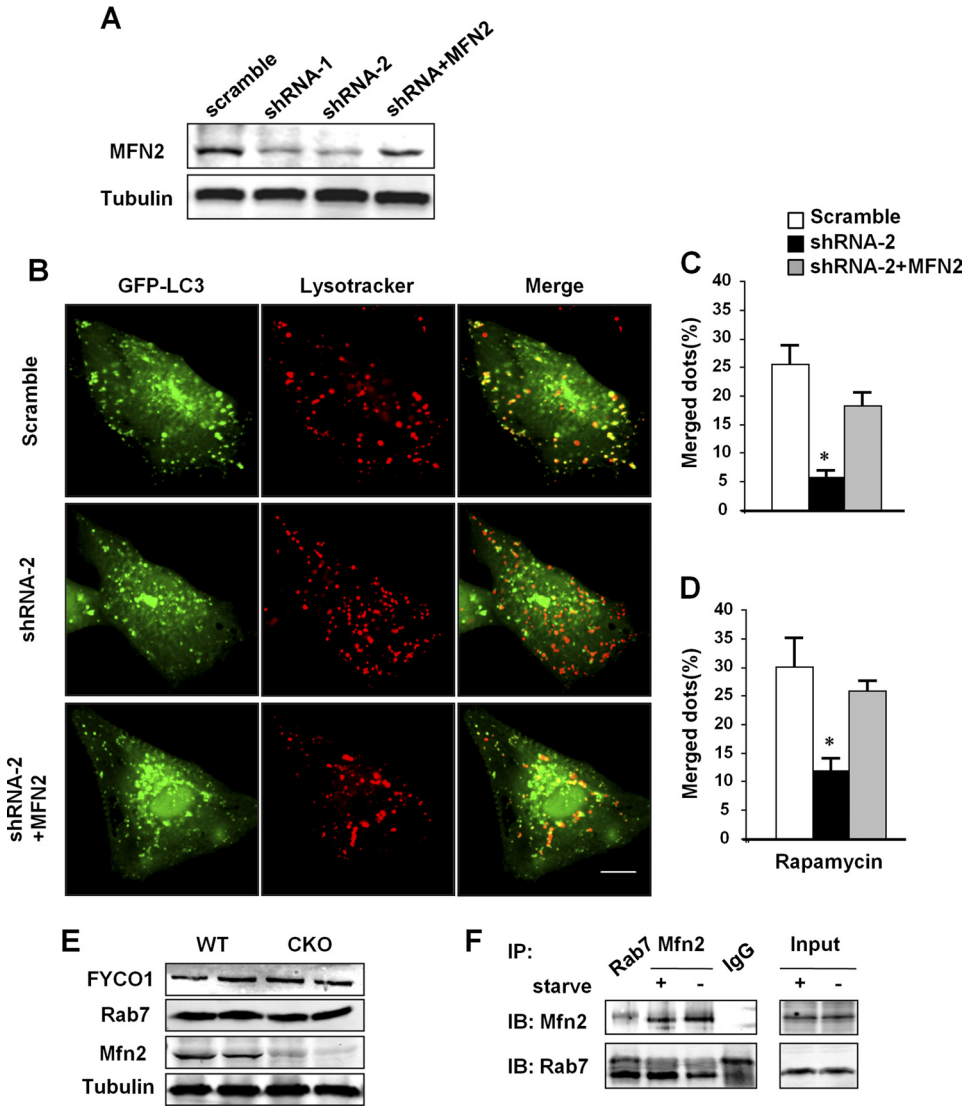

FIGURE 4. **Regulation of autophagosome-lysosome fusion by MFN2.** *A,* Western blotting showing MFN2 protein levels in neonatal cardiomyocytes transfected with adenovirus containing scrambled RNA, MFN2 shRNA1, MFN2 shRAN2, or MFN2 shRNA2 co-transfected adenovirus containing MFN2 cDNA. *B,* confocal images of neonatal cardiomyocytes co-transfected with Ad-GFP-LC3 and indicated adenovirus for 60 h and then loaded with LysoTracker™ red. *Scale bar,* 10 μm. *C,* percentages of LC3 dots merged with lysosomal dots in total LC3 dots in neonatal cardiomyocytes in *B* or *D* in the presence of rapamycin. $n = 35$ cells from three independent experiments. *, significant difference between scrambled and MFN2 knockdown neonatal cardiomyocytes. *E,* expression levels of FYCO1, RAB7, and MFN2 in wild-type and CKO hearts. Tubulin was used as loading control. *F,* whole heart lysates from mice with or without starvation were immunoprecipitated with anti-RAB7 or anti-MFN2 and analyzed with MFN2 or RAB7 antibodies, respectively. IgG was used as negative immunoprecipitation control. *IP,* immunoprecipitation; *IB,* immunoblot.

impairment on lipid metabolism in cardiomyocytes. Staining with BODYPI 493/503, a lipid droplet indicator showing lipid storage, displayed different patterns in wild-type and MFN2 knock-out cardiomyocytes, with small lipid droplets uniformly distributed in wild-type cells but heterogeneous lipid drops in MFN2-depleted cells (Fig. 5*A*), reflecting defective lipid metabolism possibly due to decreased autophagosome removal (44). In addition, we assessed the accumulation of lipofuscin granules, which indicates inhibited autophagy (45–47). The MFN2 CKO mouse heart had more lipofuscin granules than the wild-type control heart, as shown by both periodic acid-Schiff staining (Fig. 5*B*) and TEM data (Fig. 5*C*). Consistently, confocal imaging of isolated cardiomyocytes from MFN2 CKO mice, at 488 nm excitation, showed increased numbers of autofluorescent particles, a known feature of lipofuscin (data not shown). We then measured the mitochondrial respiratory control ratio, a critical feature of mitochondrial integrity with respect to the coupling of oxidation and phosphorylation, and we found a 35.2% decrease in cardiomyocytes from MFN2 CKO hearts, compared with that in wild-type hearts (Fig. 5*D*). The decreased mitochondrial respiratory control ratio was primarily caused by a 30.5% decrease in state III respiration, although the state IV oxygen consumption was unaltered between MFN2 CKO and control hearts (Fig. 5*E*), indicating that MFN2 deficiency in cardiomyocytes leads to decreased mitochondrial oxidative phosphorylation without damaging mitochondrial membrane integrity. Together, our results suggest that depletion of MFN2 in the heart leads to an overall depression of metabolic functions at both the cellular and mitochondrial levels.

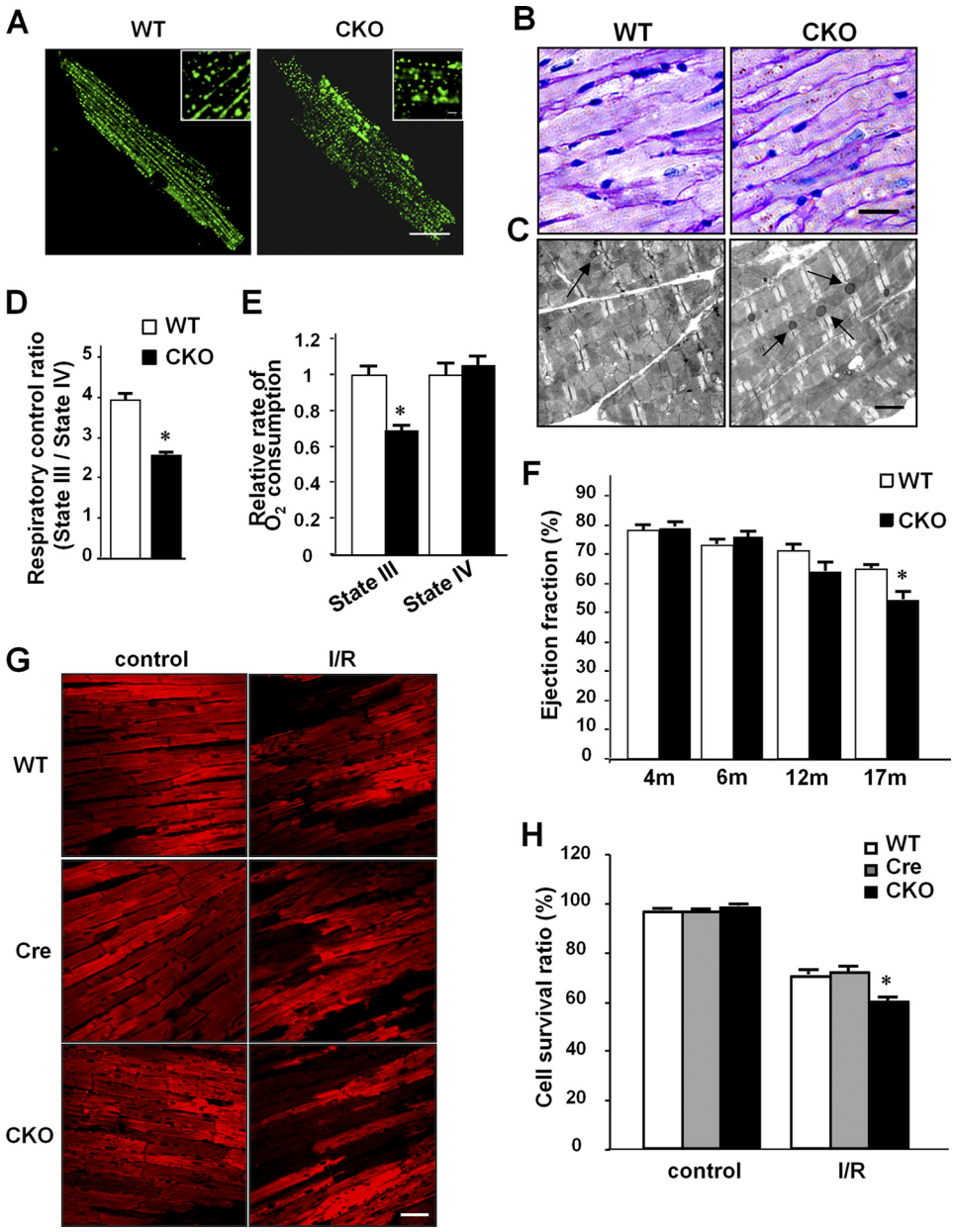

FIGURE 5. **Cell metabolism and cardiac function of MFN2 CKO mice.** *A,* BODIPY 493/503 staining for lipid droplets in isolated wild-type and CKO cardiomyocytes from 4-month-old mice. *Insets* show magnified droplets. *Scale bar,* 20 μm; *inset scale bar,* 2 μm. *B,* periodic acid-Schiff staining (*scale bar,* 50 μm); *C,* TEM (*scale bar,* 2 μm) for lipofuscin in wild-type and CKO hearts. *D,* mitochondrial respiratory control ratios in mitochondria isolated from wild-type and CKO hearts. *E,* state III O_2 consumption and state IV O_2 consumption. $n = 6$ pairs of mice at 4 months of age. *F,* echocardiogram measurements of cardiac function reflected by ejection fraction from MFN2 CKO mice and control littermates at 4, 6, 12 and 17 months of age. $n = 18$ pairs. *G,* representative confocal images of mitochondrial $\Delta\psi_m$ stained by tetramethylrhodamine methyl ester in Langendorff-perfused hearts before or after I/R stress from 6-month-old MFN2 CKO, *Mfn2* littermate control (WT), and *Mfn2*$^{+/+}$ *Mlc2v*-Cre (Cre) mice. *Scale bar,* 50 μm. *H,* statistics of percentages of cardiomyocytes maintaining $\Delta\psi_m$ before or after I/R stress in perfused mouse hearts, at 6 months of age. $n = 4$ hearts with 200 image frames for each group. *, significant difference between MFN2 CKO and littermate control or *Mlc2v*-Cre control.

Interestingly, although cellular and mitochondrial metabolism was markedly disturbed in cardiomyocytes from MFN2 CKO mice as early as 4 months old, echocardiographic analysis revealed unchanged cardiac function in these mice until the age of 17 months (Fig. 5*F* and supplemental Fig. S4*A*). Beginning from 17 months, however, MFN2 CKO mice displayed a significant decrease in left ventricular systolic function, as evidenced by a decrease of ejection fraction from 65.0 to 54.8% and fractional shortening from 30.8 to 25.0% in control and MFN2 CKO mice, respectively (Fig. 5*F* and supplemental Fig. S4*A*). These data point to a functional reserve of cardiac mitochondria in MFN2 CKO mice at ages younger than 17 months and an overtly depressed cardiac function in aging mice.

To further explore this late onset of the cardiac phenotype, we subjected MFN2 CKO and control littermate hearts to ischemia-reperfusion stress, as a means of unmasking the possible loss in functional reserve. Loss of mitochondrial membrane potential ($\Delta\Psi$m) as assessed by *ex vivo* confocal measurement of a $\Delta\Psi$m indicator, tetramethylrhodamine methyl ester fluorescence, was taken as an index of cardiomyocyte damage

(48). MFN2 CKO and control littermates at 4 months of age showed no difference in the number of cardiomyocytes that lost ΔΨm after a 30-min ischemia followed by a 30-min reperfusion (35.2% in CKO *versus* 31.2% in control littermates; supplemental Fig. S4*C*). However, ischemia-reperfusion resulted in a greater loss of ΔΨm in cardiomyocytes from MFN2 CKO mice than littermate controls and *Mlc2v*-Cre controls at the age of 6 months (42% in CKO *versus* 29.9% in control littermates and 28.5% in *Mlc2v*-Cre controls; Fig. 5, *G* and *H*), and even more loss of cardiomyocytes in MFN2 CKO mice at the age of 12 months (68.6% in CKO *versus* 31.7% in control littermates) (supplemental Fig. S4, *B* and *C*), suggesting a progressive loss of functional reserve in the MFN2 CKO mouse heart.

DISCUSSION

In this study, we demonstrated a novel role of MFN2 in regulating cardiac function through mediating the autophagic process mainly at the phase of autophagosome-lysosome fusion. Several lines of evidence are provided to support our hypothesis. First, TEM revealed extensive accumulation of autophagic vacuoles in the MFN2-deficient mouse heart. Increased protein levels of LC3-II and p62, autophagic markers, further pointed to alteration of the autophagic process by MFN2 knock-out. Second, the MFN2 knock-out heart retained a relatively normal capacity for autophagosome and lysosome formation in response to ischemia-reperfusion stress but failed to respond to blockade of autophagosome-lysosome fusion, suggesting an impairment of autophagosome degradation. Third, MFN2 interacted with RAB7, a protein that functions in the maturation of late autophagosomes, and starvation further increased the interaction of MFN2 with RAB7. Moreover, knockdown of MFN2 by shRNA impaired, and co-expression of MFN2 restored, autophagosome-lysosome fusion in neonatal cardiomyocytes. Finally, MFN2 depletion resulted in a decreased mitochondrial respiratory control ratio, defective lipid metabolism, and the accumulation of lipofuscin granules in cardiomyocytes; this may at least be due in part to impaired autophagic degradation and the consequent failure to restore cellular homeostasis.

Autophagy is an intracellular bulk degradation process important for cell survival and death, yet whether and how mitochondria regulate autophagy in the heart are still open questions. This study provides evidence that MFN2 in the heart is profoundly involved in the regulation of autophagy. MFN2 impacted on the autophagic process at least at two steps, regulating autophagic activity and mediating the maturation of autophagosomes. Both ER stress (Fig. 3) and dysfunctional mitochondria (Fig. 5) in response to MFN2 depletion may contribute to the activation of autophagy. ER stress is known to be a strong inducer of autophagy, and moreover, the stressed ER itself is autophagosomal cargo (49, 50). A previous study showed that MFN2 resides on ER membrane as well as mitochondrial membrane, regulating local calcium homeostasis and the environment inside the ER (19). Although the molecular mechanisms underlying the MFN2-related ER stress need further investigation, one speculation is that disturbed communication of ER with mitochondria and increased ER calcium content (19, 25) contribute to this process. In addition, the deficiency of MFN2 damaged the mitochondrial respiration capacity; the dysfunctional mitochondria and the subsequently decreased energy supply may serve as another initiator of the autophagic response in MFN2 CKO mouse heart.

The dynamic characteristics of autophagosome formation and their clearance by lysosomal fusion indicate that the presence of numerous autophagosomes in the MFN2-deficient heart reflects either an increase in formation or a decrease in clearance. Interestingly, although MFN2-null hearts retained considerable intact capacities for autophagosome and lysosome formation in response to ischemia-reperfusion stress, they exhibited impaired autophagosome-lysosome fusion even in the absence of the lysosome inhibitors NH_4Cl and pepstatin A (Fig. 2). It is noteworthy that inhibiting autophagosome-lysosome fusion in control mouse heart increased the LC3-II protein to a level comparable with that of the MFN2-null heart at basal levels, suggesting that impaired autophagosome-lysosome fusion, but not increased autophagic flux, contributes primarily to the extensive accumulation of autophagosomes by MFN2 depletion in the heart. Although MFN2 resides not only on mitochondrial membrane but also on ER membrane and depletion of MFN2 triggered ER stress signals which may induce enhanced autophagosome formation, ER stress *per se* did not block the fusion of autophagosomes with lysosomes as shown by the unaltered ratio of autophagosomes merging with lysosomes in the presence of an ER stressor (Fig. 3*F*). Because the ER is the main origin of autophagosomal membrane (10, 49–51), we speculated that MFN2 from ER membrane is present in the autophagosomal membrane to act as an adaptor to mediate the maturation of autophagosomes, and this was supported by the finding that MFN2 interacted with Rab7. Moreover, the restoration of autophagosome-lysosome fusion by the expression of MFN2 in cardiomyocytes further confirmed the critical role of MFN2 in regulating autophagosome maturation (Fig. 4).

In mammalian cells, MFN1 and MFN2 regulate outer mitochondrial membrane fusion (52), and deficiency of MFN1 or MFN2 leads to fragmentation of mitochondrial tubules, whereas overexpression of either restores mitochondrial morphology in mouse embryonic fibroblasts (53). Consistent with this, a recent study reported that combined ablation of MFN1/MFN2 in adult mouse heart results in fragmented mitochondria and decreased mitochondrial function, suggesting that mitochondrial fusion is essential for cardiac function (25). In contrast, cardiac MFN1 knock-out mice have normal cardiac function, although with smaller mitochondria; moreover, MFN1-deficient cardiomyocytes show improved viability in response to reactive oxygen species challenge (54). A recent study by Papanicolaou *et al.* (26) reported that MFN2 depletion in the heart leads to modest myocyte hypertrophy, mild left ventricular dysfunction, and enlarged subsarcolemmal mitochondria with a lower mitochondrial membrane potential but normal respiration. Interestingly, MFN2-deficient mitochondria show delayed mitochondrial permeability transition pore opening, which in turn protects cells against death-inducing stimuli (26). In this study, we found similarly enlarged mitochondria (supplemental Fig. S3), and mice displayed no cardiac phenotype at base line when less than 4 months old. However,

in contrast we found abnormal mitochondrial and cellular functions. Most strikingly, MFN2 depletion in cardiomyocytes caused the accumulation of autophagosomes due to impairment of autophagosome-lysosome fusion. The MFN2-null heart showed gradually increased vulnerability to ischemia-reperfusion injury and late onset cardiac dysfunction (Fig. 5 and supplemental Fig. S4). The discrepancy between the work of Papanicolaou *et al.* (26) and ours in terms of cardiac function could be due to differences in the location and timing of MFN2 deletion, the genetic background, and the ages of the mice used in these studies. For instance, the Cre mice used by the two groups were driven by distinct cardiac-specific promoters. The Cre driven by *α-MHC* is expressed in both atria and ventricles (55), whereas the Cre driven by *Mlc2v* is expressed only in the ventricles (56), leading to different knock-out patterns in the heart, which may subsequently cause disparate phenotypes.

MFN2 is crucial to the maintenance of mitochondrial metabolism, such as $\Delta\Psi$m, glucose oxidation, and cell respiration, and repression of MFN2 contributes to the metabolic defects associated with obesity (20). A link between MFN2 and components of the mitochondrially encoded oxidative phosphorylation has been reported in neuropathy (18), consistent with the observation that decreased MFN2 causes an evident inhibition of the expression of complexes I– III and V (57), indicating that MFN2 in the heart regulates cellular and mitochondrial functions in a mitochondrial fusion-independent manner (4). In this study, we found that MFN2 knock-out in the heart led to abnormal accumulation of autophagosomes (Fig. 1) and decreased mitochondrial and cellular metabolism as early as 4 months of age (Fig. 5, *A–E*), and the heart showed increased vulnerability to ischemia-reperfusion stress from 6 months of age (Fig. 5, *G* and H, and supplemental Fig. S4, *B* and *C*), and significant cardiac dysfunction appeared at 17 months of age (Fig. 5*F* and supplemental Fig. S4*A*). Although autophagy enhanced by ischemia-reperfusion stress or during chronic heart failure has either protective or deleterious effects, depending on the trigger signals (58, 59), impaired autophagosome degradation is associated with the development of cardiac myopathy (60).

In summary, our data have shown that, in addition to its role in regulating mitochondrial fusion, MFN2 is required for the clearance of damaged organelles as well as the maintenance of normal cell function in the heart. MFN2 deficiency causes autophagosome accumulation due to retarded degradation by autophagy in cardiomyocytes, and it disturbs mitochondrial structure and metabolism, which undermine cardiac reserve and eventually lead to enhanced cardiac vulnerability and overt dysfunction. These findings not only reveal MFN2 as a novel and essential player in cardiac autophagic regulation but also shed new light on understanding the molecular mechanisms of MFN2-associated human diseases.

Acknowledgment—We thank Dr. Iain C. Bruce for reading and editing the manuscript.

REFERENCES

1. Santel, A., Frank, S., Gaume, B., Herrler, M., Youle, R. J., and Fuller, M. T. (2003) Mitofusin-1 protein is a generally expressed mediator of mitochondrial fusion in mammalian cells. *J. Cell Sci.* **116,** 2763–2774
2. Rojo, M., Legros, F., Chateau, D., and Lombès, A. (2002) Membrane topology and mitochondrial targeting of mitofusins, ubiquitous mammalian homologs of the transmembrane GTPase Fzo. *J. Cell Sci.* **115,** 1663–1674
3. Misaka, T., Miyashita, T., and Kubo, Y. (2002) Primary structure of a dynamin-related mouse mitochondrial GTPase and its distribution in brain, subcellular localization, and effect on mitochondrial morphology. *J. Biol. Chem.* **277,** 15834–15842
4. Liesa, M., Palacín, M., and Zorzano, A. (2009) Mitochondrial dynamics in mammalian health and disease. *Physiol. Rev.* **89,** 799–845
5. Cipolat, S., Martins de Brito, O., Dal Zilio, B., and Scorrano, L. (2004) OPA1 requires mitofusin 1 to promote mitochondrial fusion. *Proc. Natl. Acad. Sci. U.S.A.* **101,** 15927–15932
6. Twig, G., Elorza, A., Molina, A. J., Mohamed, H., Wikstrom, J. D., Walzer, G., Stiles, L., Haigh, S. E., Katz, S., Las, G., Alroy, J., Wu, M., Py, B. F., Yuan, J., Deeney, J. T., Corkey, B. E., and Shirihai, O. S. (2008) Fission and selective fusion govern mitochondrial segregation and elimination by autophagy. *EMBO J.* **27,** 433–446
7. Gomes, L. C., and Scorrano, L. (2008) High levels of Fis1, a pro-fission mitochondrial protein, trigger autophagy. *Biochim. Biophys. Acta* **1777,** 860–866
8. Gomes, L. C., Di Benedetto, G., and Scorrano, L. (2011) During autophagy mitochondria elongates are spared from degradation and sustain cell viability. *Nat. Cell Biol.* **13,** 589–598
9. Narendra, D., Tanaka, A., Suen, D. F., and Youle, R. J. (2008) Parkin is recruited selectively to impaired mitochondria and promotes their autophagy. *J. Cell Biol.* **183,** 795–803
10. Hailey, D. W., Rambold, A. S., Satpute-Krishnan, P., Mitra, K., Sougrat, R., Kim, P. K., and Lippincott-Schwartz, J. (2010) Mitochondria supply membranes for autophagosome biogenesis during starvation. *Cell* **141,** 656–667
11. Bing, R. J., Siegel, A., Ungar, I., and Gilbert, M. (1954) Metabolism of the human heart. II. Studies on fat, ketone, and amino acid metabolism. *Am. J. Med.* **16,** 504–515
12. Suzuki, S. W., Onodera, J., and Ohsumi, Y. (2011) Starvation-induced cell death in autophagy-defective yeast mutants is caused by mitochondria dysfunction. *PLoS One* **6,** e17412
13. Chan, D. C. (2006) Mitochondria. Dynamic organelles in disease, aging, and development. *Cell* **125,** 1241–1252
14. Karbowski, M., and Youle, R. J. (2003) Dynamics of mitochondrial morphology in healthy cells and during apoptosis. *Cell Death Differ.* **10,** 870–880
15. Yaffe, M. P. (1999) The machinery of mitochondrial inheritance and behavior. *Science* **283,** 1493–1497
16. Birkedal, R., Shiels, H. A., and Vendelin, M. (2006) Three-dimensional mitochondrial arrangement in ventricular myocytes. From chaos to order. *Am. J. Physiol. Cell Physiol.* **291,** C1148–C1158
17. Kijima, K., Numakura, C., Izumino, H., Umetsu, K., Nezu, A., Shiiki, T., Ogawa, M., Ishizaki, Y., Kitamura, T., Shozawa, Y., and Hayasaka, K. (2005) Mitochondrial GTPase mitofusin 2 mutation in Charcot-Marie-Tooth neuropathy type 2A. *Hum. Genet.* **116,** 23–27
18. Züchner, S., Mersiyanova, I. V., Muglia, M., Bissar-Tadmouri, N., Rochelle, J., Dadali, E. L., Zappia, M., Nelis, E., Patitucci, A., Senderek, J., Parman, Y., Evgrafov, O., Jonghe, P. D., Takahashi, Y., Tsuji, S., Pericak-Vance, M. A., Quattrone, A., Battaloglu, E., Polyakov, A. V., Timmerman, V., Schröder, J. M., Vance, J. M., and Battologlu, E. (2004) Mutations in the mitochondrial GTPase mitofusin 2 cause Charcot-Marie-Tooth neuropathy type 2A. *Nat. Genet.* **36,** 449–451
19. de Brito, O. M., and Scorrano, L. (2008) Mitofusin 2 tethers endoplasmic reticulum to mitochondria. *Nature* **456,** 605–610
20. Bach, D., Pich, S., Soriano, F. X., Vega, N., Baumgartner, B., Oriola, J., Daugaard, J. R., Lloberas, J., Camps, M., Zierath, J. R., Rabasa-Lhoret, R., Wallberg-Henriksson, H., Laville, M., Palacín, M., Vidal, H., Rivera, F., Brand, M., and Zorzano, A. (2003) Mitofusin-2 determines mitochondrial network architecture and mitochondrial metabolism. A novel regulatory mechanism altered in obesity. *J. Biol. Chem.* **278,** 17190–17197
21. Chen, H., Vermulst, M., Wang, Y. E., Chomyn, A., Prolla, T. A., McCaffery, J. M., and Chan, D. C. (2010) Mitochondrial fusion is required for mtDNA stability in skeletal muscle and tolerance of mtDNA mutations. *Cell* **141,**

280–289
22. Chen, K. H., Guo, X., Ma, D., Guo, Y., Li, Q., Yang, D., Li, P., Qiu, X., Wen, S., Xiao, R. P., and Tang, J. (2004) Dysregulation of HSG triggers vascular proliferative disorders. *Nat. Cell Biol.* **6,** 872–883
23. Shen, T., Zheng, M., Cao, C., Chen, C., Tang, J., Zhang, W., Cheng, H., Chen, K. H., and Xiao, R. P. (2007) Mitofusin-2 is a major determinant of oxidative stress-mediated heart muscle cell apoptosis. *J. Biol. Chem.* **282,** 23354–23361
24. Chen, H., Detmer, S. A., Ewald, A. J., Griffin, E. E., Fraser, S. E., and Chan, D. C. (2003) Mitofusins Mfn1 and Mfn2 coordinately regulate mitochondrial fusion and are essential for embryonic development. *J. Cell Biol.* **160,** 189–200
25. Chen, Y., Liu, Y., and Dorn, G. W., 2nd (2011) Mitochondrial fusion is essential for organelle function and cardiac homeostasis. *Circ. Res.* **109,** 1327–1331
26. Papanicolaou, K. N., Khairallah, R. J., Ngoh, G. A., Chikando, A., Luptak, I., O'Shea, K. M., Riley, D. D., Lugus, J. J., Colucci, W. S., Lederer, W. J., Stanley, W. C., and Walsh, K. (2011) Mitofusin-2 maintains mitochondrial structure and contributes to stress-induced permeability transition in cardiac myocytes. *Mol. Cell. Biol.* **31,** 1309–1328
27. Guo, X., Chen, K. H., Guo, Y., Liao, H., Tang, J., and Xiao, R. P. (2007) Mitofusin 2 triggers vascular smooth muscle cell apoptosis via mitochondrial death pathway. *Circ. Res.* **101,** 1113–1122
28. Zheng, M., and Xiao, R. P. (2010) Role of mitofusin 2 in cardiovascular oxidative injury. *J. Mol. Med.* **88,** 987–991
29. Zheng, M., Cheng, H., Li, X., Zhang, J., Cui, L., Ouyang, K., Han, L., Zhao, T., Gu, Y., Dalton, N. D., Bang, M. L., Peterson, K. L., and Chen, J. (2009) Cardiac specific ablation of Cypher leads to a severe form of dilated cardiomyopathy with premature death. *Hum. Mol. Genet.* **18,** 701–713
30. Cheng, H., Lederer, W. J., and Cannell, M. B. (1993) Calcium sparks. Elementary events underlying excitation-contraction coupling in heart muscle. *Science* **262,** 740–744
31. Amiott, E. A., Lott, P., Soto, J., Kang, P. B., McCaffery, J. M., DiMauro, S., Abel, E. D., Flanigan, K. M., Lawson, V. H., and Shaw, J. M. (2008) Mitochondrial fusion and function in Charcot-Marie-Tooth type 2A patient fibroblasts with mitofusin 2 mutations. *Exp. Neurol.* **211,** 115–127
32. Tanhauser, S. M., and Laipis, P. J. (1995) Multiple deletions are detectable in mitochondrial DNA of aging mice. *J. Biol. Chem.* **270,** 24769–24775
33. Wallace, D. C. (1999) Mitochondrial diseases in man and mouse. *Science* **283,** 1482–1488
34. Kabeya, Y., Mizushima, N., Ueno, T., Yamamoto, A., Kirisako, T., Noda, T., Kominami, E., Ohsumi, Y., and Yoshimori, T. (2000) LC3, a mammalian homologue of yeast Apg8p, is localized in autophagosome membranes after processing. *EMBO J.* **19,** 5720–5728
35. Klionsky, D. J., Abeliovich, H., Agostinis, P., Agrawal, D. K., Aliev, G., Askew, D. S., Baba, M., Baehrecke, E. H., Bahr, B. A., Ballabio, A., Bamber, B. A., Bassham, D. C., Bergamini, E., Bi, X., Biard-Piechaczyk, M., Blum, J. S., Bredesen, D. E., Brodsky, J. L., Brumell, J. H., Brunk, U. T., Bursch, W., Camougrand, N., Cebollero, E., Cecconi, F., Chen, Y., Chin, L. S., Choi, A., Chu, C. T., Chung, J., Clarke, P. G., Clark, R. S., Clarke, S. G., Clavé, C., Cleveland, J. L., Codogno, P., Colombo, M. I., Coto-Montes, A., Cregg, J. M., Cuervo, A. M., Debnath, J., Demarchi, F., Dennis, P. B., Dennis, P. A., Deretic, V., Devenish, R. J., Di Sano, F., Dice, J. F., Difiglia, M., Dinesh-Kumar, S., Distelhorst, C. W., Djavaheri-Mergny, M., Dorsey, F. C., Droge, W., Dron, M., Dunn, W. A., Jr., Duszenko, M., Eissa, N. T., Elazar, Z., Esclatine, A., Eskelinen, E. L., Fesus, L., Finley, K. D., Fuentes, J. M., Fueyo, J., Fujisaki, K., Galliot, B., Gao, F. B., Gewirtz, D. A., Gibson, S. B., Gohla, A., Goldberg, A. L., Gonzalez, R., Gonzalez-Estevez, C., Gorski, S., Gottlieb, R. A., Haussinger, D., He, Y. W., Heidenreich, K., Hill, J. A., Hoyer-Hansen, M., Hu, X., Huang, W. P., Iwasaki, A., Jaattela, M., Jackson, W. T., Jiang, X., Jin, S., Johansen, T., Jung, J. U., Kadowaki, M., Kang, C., Kelekar, A., Kessel, D. H., Kiel, J. A., Kim, H. P., Kimchi, A., Kinsella, T. J., Kiselyov, K., Kitamoto, K., Knecht, E., Komatsu, M., Kominami, E., Kondo, S., Kovacs, A. L., Kroemer, G., Kuan, C. Y., Kumar, R., Kundu, M., Landry, J., Laporte, M., Le, W., Lei, H. Y., Lenardo, M. J., Levine, B., Lieberman, A., Lim, K. L., Lin, F. C., Liou, W., Liu, L. F., Lopez-Berestein, G., Lopez-Otin, C., Lu, B., Macleod, K. F., Malorni, W., Martinet, W., Matsuoka, K., Mautner, J., Meijer, A. J., Melendez, A., Michels, P., Miotto, G., Mistiaen, W. P., Mizushima, N., Mograbi, B., Monastyrska, I., Moore, M. N., Moreira, P. I., Moriyasu, Y., Motyl, T., Munz, C., Murphy, L. O., Naqvi, N. I., Neufeld, T. P., Nishino, I., Nixon, R. A., Noda, T., Nurnberg, B., Ogawa, M., Oleinick, N. L., Olsen, L. J., Ozpolat, B., Paglin, S., Palmer, G. E., Papassideri, I., Parkes, M., Perlmutter, D. H., Perry, G., Piacentini, M., Pinkas-Kramarski, R., Prescott, M., Proikas-Cezanne, T., Raben, N., Rami, A., Reggiori, F., Rohrer, B., Rubinsztein, D. C., Ryan, K. M., Sadoshima, J., Sakagami, H., Sakai, Y., Sandri, M., Sasakawa, C., Sass, M., Schneider, C., Seglen, P. O., Seleverstov, O., Settleman, J., Shacka, J. J., Shapiro, I. M., Sibirny, A., Silva-Zacarin, E. C., Simon, H. U., Simone, C., Simonsen, A., Smith, M. A., Spanel-Borowski, K., Srinivas, V., Steeves, M., Stenmark, H., Stromhaug, P. E., Subauste, C. S., Sugimoto, S., Sulzer, D., Suzuki, T., Swanson, M. S., Tabas, I., Takeshita, F., Talbot, N. J., Talloczy, Z., Tanaka, K., Tanida, I., Taylor, G. S., Taylor, J. P., Terman, A., Tettamanti, G., Thompson, C. B., Thumm, M., Tolkovsky, A. M., Tooze, S. A., Truant, R., Tumanovska, L. V., Uchiyama, Y., Ueno, T., Uzcategui, N. L., van der Klei, I., Vaquero, E. C., Vellai, T., Vogel, M. W., Wang, H. G., Webster, P., Wiley, J. W., Xi, Z., Xiao, G., Yahalom, J., Yang, J. M., Yap, G., Yin, X. M., Yoshimori, T., Yu, L., Yue, Z., Yuzaki, M., Zabirnyk, O., Zheng, X., Zhu, X., and Deter, R. L. (2008) Guidelines for the use and interpretation of assays for monitoring autophagy in higher eukaryotes. *Autophagy* **4,** 151–175
36. Yorimitsu, T., and Klionsky, D. J. (2005) Autophagy. Molecular machinery for self-eating. *Cell Death Differ.* **12,** Suppl. 2, 1542–1552
37. Bjørkøy, G., Lamark, T., Brech, A., Outzen, H., Perander, M., Overvatn, A., Stenmark, H., and Johansen, T. (2005) p62/SQSTM1 forms protein aggregates degraded by autophagy and has a protective effect on huntingtin-induced cell death. *J. Cell Biol.* **171,** 603–614
38. Hamacher-Brady, A., Brady, N. R., Logue, S. E., Sayen, M. R., Jinno, M., Kirshenbaum, L. A., Gottlieb, R. A., and Gustafsson, A. B. (2007) Response to myocardial ischemia/reperfusion injury involves Bnip3 and autophagy. *Cell Death Differ.* **14,** 146–157
39. Ganley, I. G., Wong, P. M., Gammoh, N., and Jiang, X. (2011) Distinct autophagosomal-lysosomal fusion mechanism revealed by thapsigargin-induced autophagy arrest. *Mol. Cell* **42,** 731–743
40. Gutierrez, M. G., Munafó, D. B., Berón, W., and Colombo, M. I. (2004) Rab7 is required for the normal progression of the autophagic pathway in mammalian cells. *J. Cell Sci.* **117,** 2687–2697
41. Jäger, S., Bucci, C., Tanida, I., Ueno, T., Kominami, E., Saftig, P., and Eskelinen, E. L. (2004) Role for Rab7 in maturation of late autophagic vacuoles. *J. Cell Sci.* **117,** 4837–4848
42. Pankiv, S., Alemu, E. A., Brech, A., Bruun, J. A., Lamark, T., Overvatn, A., Bjørkøy, G., and Johansen, T. (2010) FYCO1 is a Rab7 effector that binds to LC3 and PI3P to mediate microtubule plus end-directed vesicle transport. *J. Cell Biol.* **188,** 253–269
43. Rabinowitz, J. D., and White, E. (2010) Autophagy and metabolism. *Science* **330,** 1344–1348
44. Singh, R., Kaushik, S., Wang, Y., Xiang, Y., Novak, I., Komatsu, M., Tanaka, K., Cuervo, A. M., and Czaja, M. J. (2009) Autophagy regulates lipid metabolism. *Nature* **458,** 1131–1135
45. Inuzuka, Y., Okuda, J., Kawashima, T., Kato, T., Niizuma, S., Tamaki, Y., Iwanaga, Y., Yoshida, Y., Kosugi, R., Watanabe-Maeda, K., Machida, Y., Tsuji, S., Aburatani, H., Izumi, T., Kita, T., and Shioi, T. (2009) Suppression of phosphoinositide 3-kinase prevents cardiac aging in mice. *Circulation* **120,** 1695–1703
46. Stroikin, Y., Dalen, H., Lööf, S., and Terman, A. (2004) Inhibition of autophagy with 3-methyladenine results in impaired turnover of lysosomes and accumulation of lipofuscin-like material. *Eur. J. Cell Biol.* **83,** 583–590
47. Terman, A., Dalen, H., Eaton, J. W., Neuzil, J., and Brunk, U. T. (2004) Aging of cardiac myocytes in culture. Oxidative stress, lipofuscin accumulation, and mitochondrial turnover. *Ann. N.Y. Acad. Sci.* **1019,** 70–77
48. Wang, X., Xie, W., Zhang, Y., Lin, P., Han, L., Han, P., Wang, Y., Chen, Z., Ji, G., Zheng, M., Weisleder, N., Xiao, R. P., Takeshima, H., Ma, J., and Cheng, H. (2010) Cardioprotection of ischemia/reperfusion injury by cholesterol-dependent MG53-mediated membrane repair. *Circ. Res.* **107,** 76–83
49. Axe, E. L., Walker, S. A., Manifava, M., Chandra, P., Roderick, H. L., Habermann, A., Griffiths, G., and Ktistakis, N. T. (2008) Autophagosome formation from membrane compartments enriched in phosphatidylinositol

3-phosphate and dynamically connected to the endoplasmic reticulum. *J. Cell Biol.* **182,** 685–701
50. Hayashi-Nishino, M., Fujita, N., Noda, T., Yamaguchi, A., Yoshimori, T., and Yamamoto, A. (2009) A subdomain of the endoplasmic reticulum forms a cradle for autophagosome formation. *Nat. Cell Biol.* **11,** 1433–1437
51. McEwan, D. G., and Dikic, I. (2010) Not all autophagy membranes are created equal. *Cell* **141,** 564–566
52. Koshiba, T., Detmer, S. A., Kaiser, J. T., Chen, H., McCaffery, J. M., and Chan, D. C. (2004) Structural basis of mitochondrial tethering by mitofusin complexes. *Science* **305,** 858–862
53. Detmer, S. A., and Chan, D. C. (2007) Complementation between mouse Mfn1 and Mfn2 protects mitochondrial fusion defects caused by CMT2A disease mutations. *J. Cell Biol.* **176,** 405–414
54. Papanicolaou, K. N., Ngoh, G. A., Dabkowski, E. R., O'Connell, K. A., Ribeiro, R. F., Stanley, W. C., and Walsh, K. (2011) *Am. J. Physiol. Heart Circ. Physiol.* 302, H167–H179
55. Agah, R., Frenkel, P. A., French, B. A., Michael, L. H., Overbeek, P. A., and Schneider, M. D. (1997) Gene recombination in postmitotic cells. Targeted expression of Cre recombinase provokes cardiac restricted, site-specific rearrangement in adult ventricular muscle *in vivo*. *J. Clin. Invest.* **100,** 169–179
56. Minamisawa, S., Gu, Y., Ross, J., Jr., Chien, K. R., and Chen, J. (1999) A post-transcriptional compensatory pathway in heterozygous ventricular myosin light chain 2-deficient mice results in lack of gene dosage effect during normal cardiac growth or hypertrophy. *J. Biol. Chem.* **274,** 10066–10070
57. Pich, S., Bach, D., Briones, P., Liesa, M., Camps, M., Testar, X., Palacín, M., and Zorzano, A. (2005) The Charcot-Marie-Tooth type 2A gene product, Mfn2, up-regulates fuel oxidation through expression of OXPHOS system. *Hum. Mol. Genet.* **14,** 1405–1415
58. Matsui, Y., Takagi, H., Qu, X., Abdellatif, M., Sakoda, H., Asano, T., Levine, B., and Sadoshima, J. (2007) Distinct roles of autophagy in the heart during ischemia and reperfusion. Roles of AMP-activated protein kinase and Beclin 1 in mediating autophagy. *Circ. Res.* **100,** 914–922
59. Sciarretta, S., Hariharan, N., Monden, Y., Zablocki, D., and Sadoshima, J. (2011) Is autophagy in response to ischemia and reperfusion protective or detrimental for the heart? *Pediatr. Cardiol.* **32,** 275–281
60. Tanaka, Y., Guhde, G., Suter, A., Eskelinen, E. L., Hartmann, D., Lüllmann-Rauch, R., Janssen, P. M., Blanz, J., von Figura, K., and Saftig, P. (2000) Accumulation of autophagic vacuoles and cardiomyopathy in LAMP-2-deficient mice. *Nature* **406,** 902–906